Carbon dioxide adsorption on metal organic framework Basolite C300

Submitted in partial fulfillment of the requirement for the award of the Degree of

Master of Technology

In

Chemical Engineering

Submitted by:

RONJISH CHUGH
(601311007)

Under the guidance of

Dr. Pramod K. Bajpai
Distinguished Professor
ChED

Dr. Haripada Bhunia
Associate Professor
ChED

Department of Chemical Engineering

THAPAR UNIVERSITY

PATIALA-147004, PUNJAB

June 2015

CERTIFICATE

This is to certify that the dissertation entitled **"Carbon dioxide adsorption on metal organic framework Basolite C300"**, is an authentic record of my own work carried out as requirements for the award of degree of master of technology in Chemical Engineering from Thapar University, Patiala, under the guidance of Dr. Pramod K. Bajpai (Distinguished Professor, ChED) and Dr. Haripada Bhunia (Associate Professor, ChED) during the academic session **Jan-June 2015**.

Date: 05/07/15

Ronjish

Ronjish Chugh

(Roll No: 601311007)

It is certified that the above statement made by the student is correct to the best of our knowledge and belief.

05-07-2015

Dr. Pramod K. Bajpai
Distinguished Professor
ChED

05/07/2015

Dr. Haripada Bhunia
Associate Professor
ChED

Countersigned by:

Dr. Raj Kumar Gupta
Head, ChED

Dr. S. S. Bhatia
Dean, Academic Affairs
Thapar University, Patiala

Acknowledgements

I am highly grateful to the authorities of **Thapar University, Patiala** for providing this opportunity to carry out my work.

I would like to express a deep sense of gratitude and thank profusely to my esteemed guides **Dr. Pramod K. Bajpai**, Distinguished Professor and **Dr. Haripada Bhunia**, Associate Professor, Department of Chemical Engineering, Thapar University, Patiala for giving me an opportunity to work under their guidance and inspiration throughout the work.

I am heartily thankful to **Dr. Raj Kumar Gupta (HOD, ChED)** for allowing me and providing me facilities to complete this work.

Somebody whose great experience put the things right way, **Ms. Chitrakshi Goel**, I am extremely thankful to her for kind help and support.

I am thankful to my beloved parents for their love and encouragement.

I am thankful to all my friends Karishma Katoch and Arghya Dutta.

Ronjish

Ronjish Chugh

Roll No- 601311007

DECLARATION

I hereby declare that the dissertation entitled **"Carbon dioxide adsorption on metal organic framework Basolite C300"** submitted by Ms. Ronjish Chugh in the fulfillment of the requirement for the award of **Master of Technology in Chemical Engineering at Thapar University, Patiala** under the guidance of **Dr. Pramod K. Bajpai**, Distinguished Professor and **Dr. Haripada Bhunia**, Associate Professor, Department of Chemical Engineering during **Jan 2015 to June 2015.**

To the best of my knowledge, the matter embodied in the project has not been submitted to any other University/Institute for the award of any degree.

Date: 05/07/15

Ronjish

Ronjish Chugh

(601311007)

ABSTRACT

Carbon dioxide has become a global concern in recent years because of its enormous increase in the atmosphere. Various efforts have been made to control and capture it. The main source of carbon dioxide emission is the combustion of fossil fuels i.e. coal, natural gas, oil. The burning of these fossil fuels releases large amounts of CO_2 into the atmosphere. It is considered as one of the major source of global warming. Carbon capture and sequestration (CCS) is the only technology that enables the capture of CO_2 from fossil fuels. One of the carbon capture technology is adsorption process. Gas separation by adsorption process is widely used, in which choice of the good adsorbent is the key for the separation. There are many adsorbent materials like activated carbons, silica gel, zeolites, activated alumina etc, which are being used to capture the carbon dioxide. Metal organic frameworks are the new class of the adsorbents, which have been investigated as the high potential adsorbents. Here, MOF used is Basolite C300 i.e. copper benzene 1,3,5-tricarboxylate (Cu-BTC MOF), it is also known as HKUST-1. In this study, carbon dioxide adsorption/desorption was investigated using temperature swing adsorption process. Breakthrough study for the adsorption of carbon dioxide on Basolite C300 was done using fixed bed reactor at different temperatures and feed concentrations. It gives the maximum adsorption at lower temperature and higher concentration. It was found that Basolite C300 has a maximum dynamic CO_2 adsorption capacity 1.45 mmol/g at 303K. Kinetic data obtained was analyzed using pseudo first order and pseudo second order models. Pseudo second order kinetic model shows the better applicability. The experimental data were analyzed by the Langmuir and Freundlich isotherm models of adsorption. The adsorption data fitted well to Langmuir isotherm model.

TABLE OF CONTENTS

LIST OF FIGURES

LIST OF TABLES

LIST OF SYMBOLS

BTC	1,2,3-benzenetricaboxylate
C	concentration of adsorbate at time t (mol /m^3)
C_o	initial feed concentration (mol/m^3)
CCS	CO_2 capture and sequestation
GHG	Greenhouse gas
IPCC	Intergovernmental panel on climate change
k	Constant for a given adsorbent and adsorbate at particular temperature
K_l	Langmuir isotherm constant (L/mg)
K_f	Freundlich constants related to adsorption capacity (L/mg)
MOFs	Metal organic frameworks
n	Adsorption intensity of adsorbents
q	Adsorbed amount (mmol/g)
SSE	Sum of square error
T	Temperature (K)
t	Time (s)
TGA	Thermo gravimetrical analysis
XRD	X-ray diffraction

Chapter-1

INTRODUCTION

Sharply increasing concentration of carbon dioxide in environment is the main reason of global warming. With increasing economic growth and industrial development, the main sources of carbon dioxide emission in the environment are coal, oil, and natural gas, which are projected to increase further in the future. However, various technologies and methods are developed for CO_2 capture and sequestration (CCS) [1]. CCS technologies that efficiently capture carbon dioxide from existing emission sources will play an important role until more major modifications can be recognized. There are three basic approaches for CO_2 separation and capture from fossil fuels (1) pre-combustion capture; (2) oxy-fuel combustion; and (3) post-combustion capture [2, 3]. In each process, there are different conditions of temperature and pressure, out of which post combustion capture has more advantages over other two approaches [4] because it can easily be installed to existing plants, integrated into new plants and has high operational flexibility. Various technologies are being used to improve the CO_2 capture; one of them is adsorption separation. Adsorption of CO_2 is one of the simplest processes that can be easily operated with a low energy requirement and high CO_2 adsorption capacity [5-8]. Therefore, it is an effective technology for the post combustion CO_2 capture [9].

In this regard, porous hybrid adsorbent known as metal organic frameworks (MOFs) have been developed. MOFs are of great interest in chemical industries because of their applications and high potential i.e. gas storage, gas purification, separations and catalysis. MOFs are made of metal ion clusters linked through organic linkers and inorganic metal nodes in a definite geometry [10-12]. They have high porosity, large surface areas, open metal sites and higher CO_2 capture capacity than that of zeolites or carbon [10]. However, various types of MOFs have been studied as gas storage materials and plenty of equilibrium adsorption data for various gases are available in published literature [13], their dynamic gas adsorption study is still new.

1.1 Carbon Capture and Sequestration (CCS)

CCS is associated with the selective capture of carbon dioxide from the power plant flue gas that must certainly be reduced if such an approach for carbon dioxide decrease is made to become feasible. The high cost primarily arises from the large energy input required for regeneration of the capture material. Indeed, carbon dioxide capture from a post-combustion flue gas using the most highly developed current technologies involving aqueous alkanol amine solutions carries an energy price of roughly 30% of the output of the power plant, most of which is associated with the liberation of the captured carbon dioxide from the captured medium. Thus, minimization of the energy input for regeneration, through fine-tuning of the thermodynamics of the interaction between carbon dioxide and the adsorbent, for example, is one of the most critical considerations in improving the energy efficiency of carbon dioxide capture.

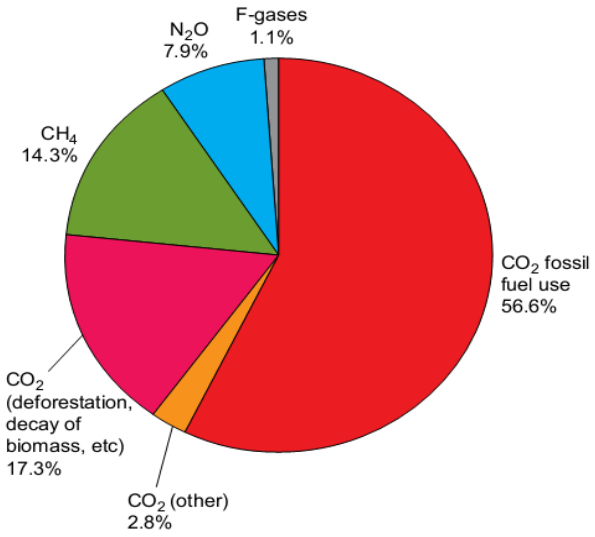

Fig. 1.1 Global greenhouse gas emission sources in 2013 [14]

As shown in Figure 1.1, the combustion of fossil fuels represents over half of the global greenhouse gas emissions [14]. Global CO_2 emissions have increased by approximately 80% over the period 1970-2013 (from 21 to 38 Gt/year), and these emission levels are projected to increase further over the next several decades owing to rise in energy

demands associated with a growing global population and economic and industrial development.

1.2 Methods of Carbon Dioxide Capture

Exploring cost-effective and scalable technologies and methods for carbon dioxide capture from power generation and industrial operation where carbon dioxide is produced on the combustion of fossil fuels is regarded as the most effective strategy in controlling anthropogenic carbon dioxide emission. Depending on the generation of carbon dioxide, several capture options and tendentious technologies have been suggested and implemented. Generally, based on the fundamental chemical processes involved in the combustion of fossil fuels, three basic carbon dioxide separation and capture options were adopted: (1) pre-combustion capture; (2) oxy-fuel combustion; and (3) post-combustion capture as shown in Fig. 1.2.

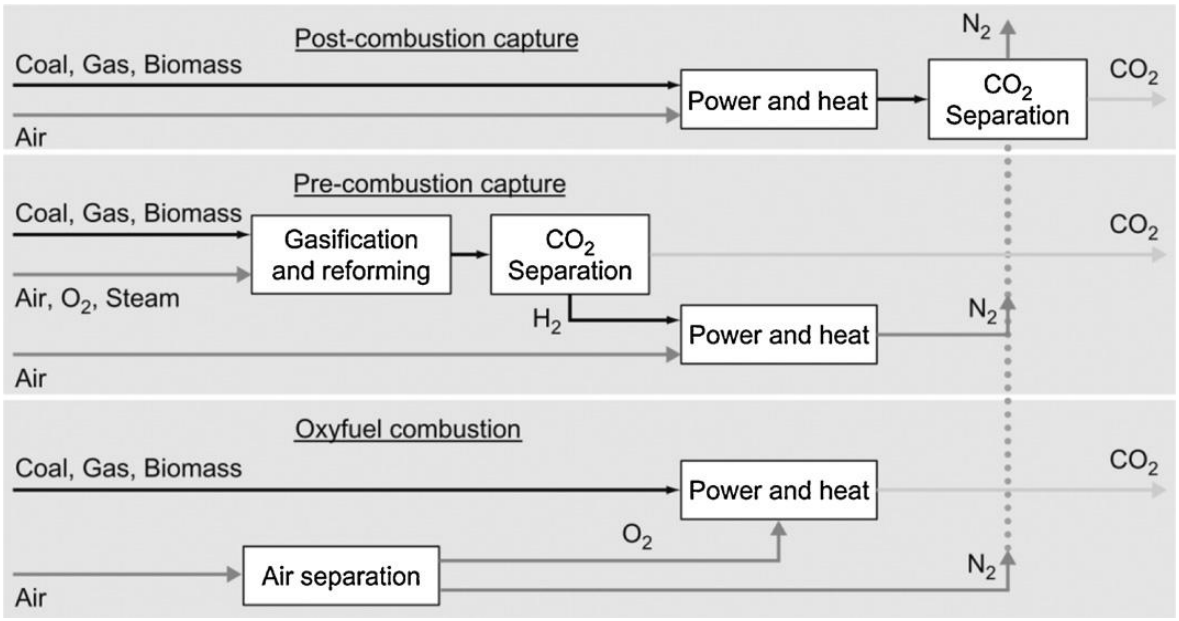

Fig 1.2 Three options for carbon dioxide capture from power generation plants [11].

1.2.1 Pre-combustion capture

Pre-combustion capture process converts fuel into a gaseous mixture of hydrogen and CO_2. The hydrogen is separated and can be burnt without producing any CO_2. The CO_2 can then be compressed for transport and storage. Pre-combustion has the advantage

of lower energy requirements, but the temperature and efficiency associated with hydrogen-rich gas turbine fuel is a big problem. More challenging issues are the enormous capital cost and the public resistance for new construction [11].

1.2.2 Oxy-fuel combustion

In this process nearly pure oxygen is required, rather than air, for the combustion of fuels; the advantage here being that the gaseous product is nearly pure carbon dioxide, which can be directly stored. The drawback of this option is the requirement of pure oxygen, which can usually be obtained by the separation of air or by other novel techniques that are available [11].

1.2.3 Post-combustion capture

Post-combustion process separates CO_2 from combustion exhaust gases. CO_2 can be captured using liquid solvent or other separation methods. In an absorption-based approach, once absorbed by the solvent, the CO_2 is released by heating to form a high purity CO_2 stream [11].

This process requires removing carbon dioxide from flue gas, comprised mainly of N_2 and carbon dioxide, before its emission into the atmosphere. It is more feasible on a short time scale because many of the proposed technologies can be enhanced to existing fossil fuel consuming power plants. Advantage of post-combustion capture is that even if the carbon dioxide capture unit is shut down for an emergency, one can still generate electricity, which is not possible with other more integrated capture methods.

1.3 Carbon Dioxide Capture Technologies

Most carbon dioxide capture technologies are not new. Specialized chemical solvents were developed more than 60 years ago to remove carbon dioxide from impure natural gas, and natural gas operations continue to use these solvents today. In addition, several power plants and other industrial plants use the same or similar solvents to recover carbon dioxide from flue gases for application in food processing and chemical industries. The selection of a technology for a given capture application depends on many factors i.e. partial pressure of carbon dioxide in the gas stream, extent of carbon dioxide recovery required, sensitivity to impurities, such as acid gases, particulates, purity of desired carbon dioxide product, capital and operating costs of the process, the cost of additives necessary to overcome fouling and corrosion, where applicable the

environmental impacts. Based upon the method of carbon dioxide removal, capture technologies can be broadly classified into various categories as shown in Fig 1.3.

The established technologies, cryogenic distillation and amine based absorption, have high (60-80%) energy penalty. These are matured technologies and scope for further improvement is limited. The challenge is to develop a technology that has lower energy penalty. In view of very large amount of CO_2 that must be captured and concentrated, the plant size and capital cost are also important considerations. Adsorption based cyclic processes are emerging as energy efficient alternatives for industrial gas separation applications. They also offer economies of scale, unlike membrane processes. Hence adsorption technology is a potential candidate to offer lower energy solution for carbon capture and sequestration and other clean energy applications.

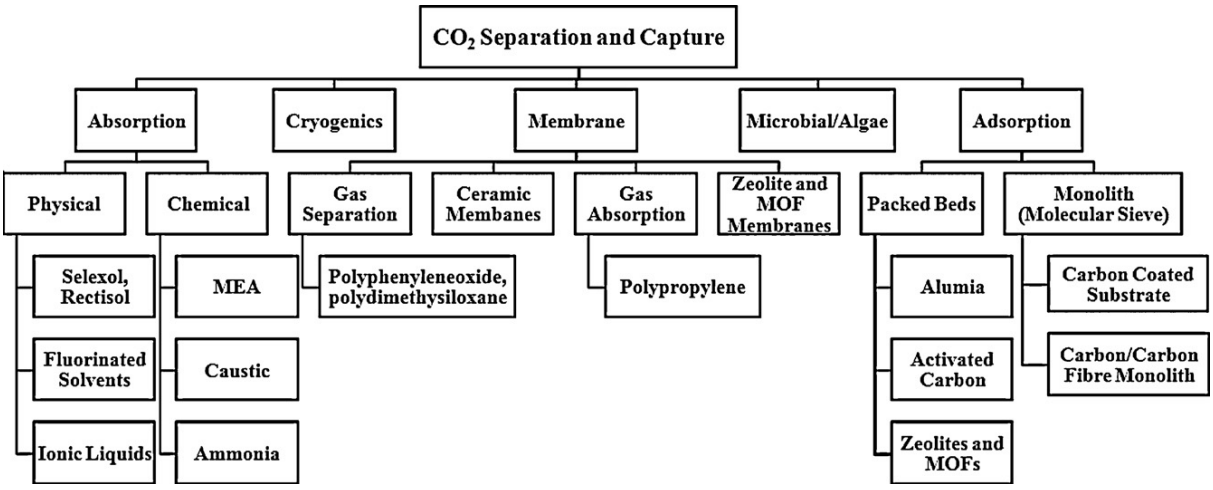

Fig. 1.3 Different technologies and associated materials for CO_2 separation and capture [15]

Adsorption separation processes are in extensive industrial use, particularly in the petrochemical industries and petroleum refining. In industries, large-scale separation of CO_2 by amine-based absorption is used but it has some weaknesses - corrosiveness, low interfacial area, requirement of pure water and high-energy cost. Alternatively, there are many adsorbent materials that have been studied for CO_2 capture such as, activated carbon, zeolites and zeolite-like materials. The porous solid provides a very high surface area or high micropore volume and it is this high surface area or micropore volume that

contributes to the high adsorptive capacity. The first major adsorbent in the adsorption industry was zeolite. Adsorption separation processes are categorized on the basis of mechanism of gas separation, namely steric, kinetic and equilibrium separations. In steric mechanism, the size and shape of the gas molecule is important. This means that only the small molecules with proper shape can disperse into the adsorbent. This effect can be seen in some zeolites with molecular sieving property. In case of kinetic separation, different molecules with different size and shape diffuse into the pores, but at different rates. None of the adsorbents fulfill the entire requirement. Thus, there is an urgent need to develop new adsorbents.

1.3.1 MOF: A new family of adsorbents

There are many physical adsorbent materials that have been considered for CO_2 capture such as, activated carbon, zeolites and zeolite-like materials, and metal organic frameworks (MOFs). However, suitable adsorbent for CO_2 capture from flue gas should satisfy several important criteria to compete with the present technologies, including:

1) high adsorption capacity
2) high selectivity
3) high regenerability

MOFs are crystalline, sponge-like materials comprised of metal-containing nodes linked by organic ligand bridges and assembled principally through strong coordination bonds [16]. MOFs have broad industrial applications because of the key attributes:

- ✓ ultrahigh porosity
- ✓ extremely large surface-areas and
- ✓ flexibility with which their structures can be varied.

They are also very robust, with high mechanical and thermal stabilities. The ability to rationally select the framework components is expected to allow the affinity of the internal pore surface toward carbon dioxide to be precisely controlled, facilitating materials properties that are optimized for the specific type of carbon dioxide capture to be performed (post-combustion capture, pre-combustion capture, or oxy-fuel combustion) and potentially even for the specific power plant in which the capture system is to be installed. For this reason, significant effort has been made in recent years in improving

the gas separation performance of metal organic frameworks, and some studies evaluating the prospects of establishing these materials in real-world carbon dioxide.

1.4 Objectives and Scope of the Work

The main objective of the present work is to measure the dynamic adsorption of CO_2 onto Basolite C300 at different temperatures and CO_2 concentrations and to study the effect of operating parameters on the breakthrough adsorption value.

1) Characterization of adsorbent for thermal stability using thermogravimetric analysis (TGA).
2) The study on kinetic adsorption performance of Basolite C300 using a fixed bed adsorption column under several experimental conditions by varying the adsorption temperature, and the feed concentration of CO_2 and observing the effects.
3) Fitting of kinetic models (pseudo first order and pseudo second order) to the adsorption data.
4) Isothermal study using the isotherm models (Langmuir and Freundlich isotherms).

Chapter-2

LITERATURE REVIEW

In several excellent reviews on CO_2 capture by adsorption [16,17], it can be understood that to develop an appropriate CO_2 capture adsorbent should satisfy (1) low-cost raw materials, (2) low heat capacity, (3) fast kinetics, (4) high CO_2 adsorption capacity, (5) high CO_2 selectivity and (6) thermal, chemical, and mechanical stabilities under extensive cycling. A variety of solid adsorbents have been proposed to take into account of their structures and compositions, adsorption mechanisms, and regeneration. Here, physical adsorption, mesoporous adsorbents metal organic framework is used for its adsorption study.

Basolite C300 is the MOF of interest for the present study. In this chapter, MOF structures and structural characterization of Cu-BTC and adsorption of gases on this material are discussed. The relevant literature on adsorption equilibrium and kinetics, and the potential of Cu-BTC in gas separation application are also discussed.

2.1 Metal Organic Frameworks

MOFs are made of metal ion clusters linked through organic linkers and inorganic metal nodes in a definite geometry [12,15,18]. They have high porosity, large surface area, open metal sites and higher CO_2 capture capacity than that of other adsorbents [4]. On development of metal organic frameworks as post combustion CO_2 capture adsorbent, relatively few reports have come into view. However various types of MOFs have been studied as gas storage materials and plenty of equilibrium adsorption data for various gases are available in published literature [19], their dynamic gas adsorption property is still new.

2.1.1 Structure of MOF

MOFs are comprised of metal-containing nodes (e.g. Al^{3+}, Cr^{3+}, Cu^{2+} or Zn^{2+}) linked by organic ligand (e.g. carboxylate, pyridyl) bridges and assembled principally through strong coordination bonds (Fig. 2.1).

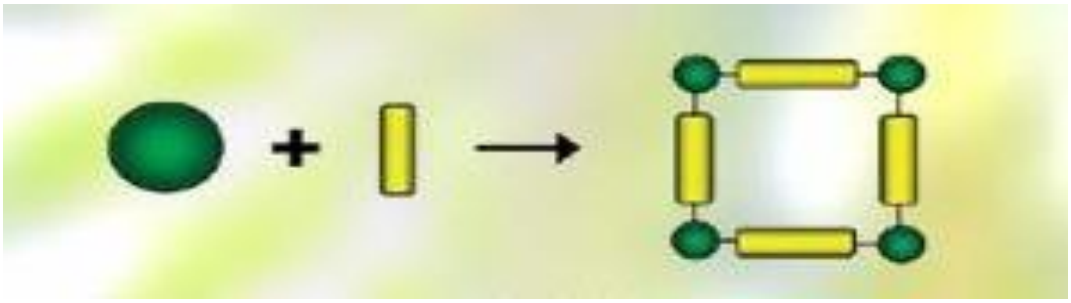

Inorganic part + linker = Metal Organic Framework (coordination polymer)

Fig. 2.1 MOF structure

MOFs are carefully selected such that their properties are maintained and showed by the product material. Its properties are robustness, high surface area (up to 5000 cm^2/g) high thermal and chemical stabilities, high void volume (55-90%), low densities (from 0.21 to 1 g/cm^3) [20], and their potential applications in gas storage, ion exchange, molecular separation, drug delivery, and heterogeneous catalysis [20,21]. This remarkable and easy tunability of MOFs is a key feature that distinguishes these materials from traditional porous materials, such as zeolites and activated carbon [22,23]. There are different types of MOFs which have been studied so far, One of the most studied metal organic frameworks is the $Cu_3(BTC)_2$ (HKUST-1) or Basolite C300.

2.2 Basolite C300

Basolite C300 is also known as HKUST-1. **Copper benzene-1,3,5-tricarboxylate** is a highly porous and crystalline. It is composed of copper(II) and trimesate ions [25]. Basolite C300 consists of dinuclear Cu^{2+} paddlewheel units and triangular 1,3,5-benzene tricarboxylate linker as shown in Fig 2.2 [24,25].

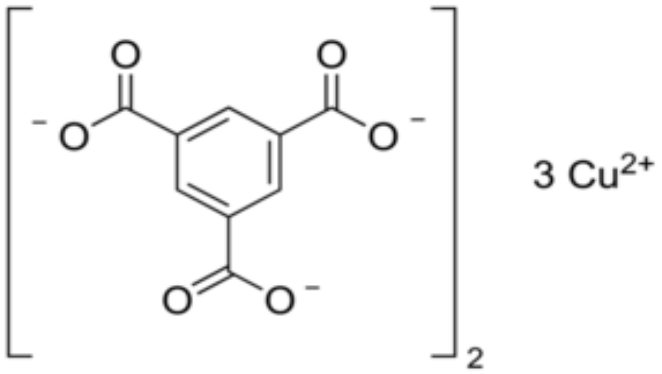

Fig. 2.2 Structure of Basolite C300

The choice of Cu-BTC is due to its high thermal stability and also it has a high surface area [26] and easily available. Its framework contains bound solvent molecules on the axial coordination sites of each Cu^{2+} metal center, which can be used to create open binding sites for guest molecules. These sites act as charge-dense point charges, which provide an opportunity for inequity of certain components of gas mixtures based on their dipole or quadrupole moment and polarity [27]. Cu-BTC is hydrophilic and can be reactivated at 150 °C [23]. Its applications include noble gas adsorption and catalysis. Some physical properties of the Basolite C300 are shown in the Table 2.1

Table 2.1 Physical properties of Basolite C300

Surface area	1500-2100 m^2/g
Particle size	15.96 μm
Bulk density	0.35 g/cm^3

2.2.1 Structure of Basolite C300

Cu-BTC is composed of metal coordination polymers having Cu acting as joints and benzene-1,3,5-tricarboxylate (BTC) ligand as the linkers. The partial positive charges on the metal sites in Cu-BTC can lead to better adsorption properties [28]. The resultant structure has big cavities and small octahedral cages. A Cu-BTC unit cell has cubic symmetry. This unit cell is formed by six side cages of octahedral shape (not symmetric) located at the vertices of the unit cell, and related by the metal centers. The octahedral

structures are formed by BTC molecules placed in alternate faces. The rest of the faces are free of molecules, forming windows that allow the access to the side cages. Therefore, in the center of the unit cell there is a nearly spherical void space of 9 Å in diameter [29]. Figure 2.3 shows the 3D structure of Cu-BTC. The main pore and side pockets are also shown.

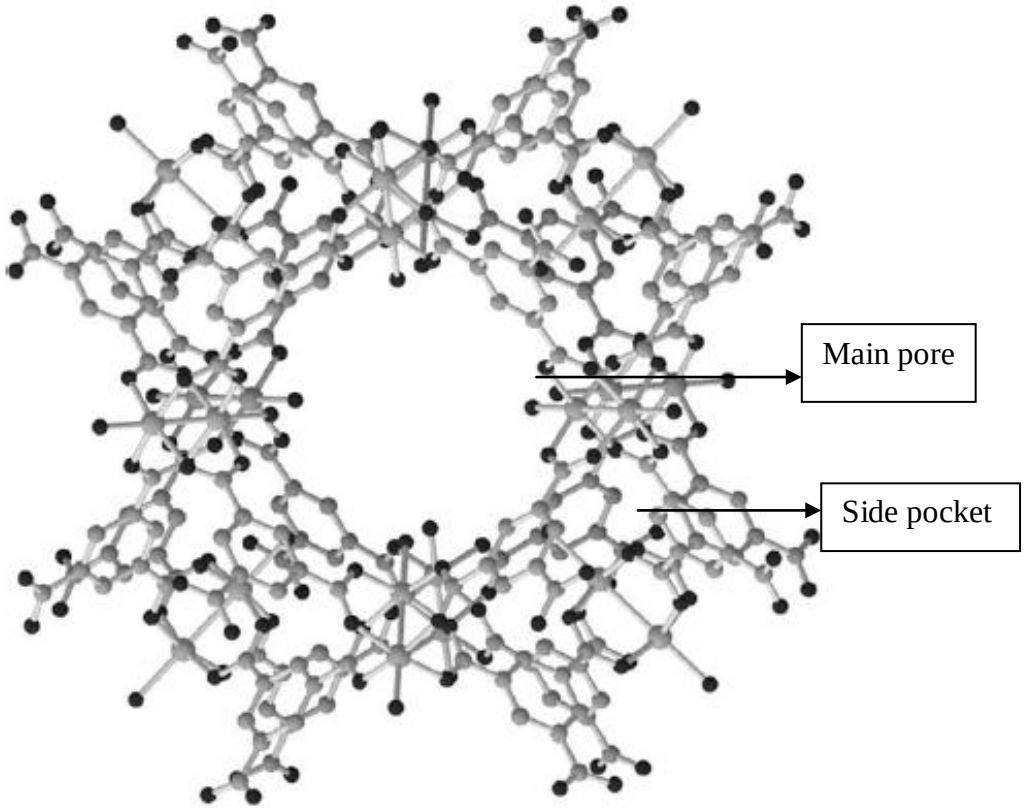

Fig. 2.3 Crystal structure of $Cu_3(BTC)_2(H_2O)_3$ [30]

2.3 CO_2 Adsorption Capacity of Different MOFs

The evaluation of new adsorbent materials for CO_2 capture applications depends on many factors, such as the adsorption capacity, selectivity and enthalpy of adsorption. However, most of MOF literature has focused onto CO_2 adsorption capacity by measuring the adsorption equilibrium rather than measuring the adsorption under dynamic fixed bed configuration.

Lots of MOFs have been investigated experimentally for CO_2 adsorption and related gas separation. The results of these experiments have been summarized in Table 2.2, which represents the adsorption capacity for MOFs at ambient temperatures, with pressures

ranging from low pressure (<1.2 bar) to atmospheric pressure in most of the cases. The adsorption isotherms measured at ambient temperature and low pressure are mainly controlled by chemical feature of the pore surface, and most of the high capacity materials are those of highly functionalized surface.

Table 2.2 CO_2 adsorption capacities of MOFs

Materials	Common Name	Temperature (K)	Pressure (bar)	Capacity (wt%)	Reference
$Zn_4O(BTB)_2$	MOF-177	298	1	3.6	31
$Mg_2(dobdc)$	Mg-MOF-74	298	1	27.2	32
$Ni_2(DOBDC)$	Ni-MOF-74	298	1	23.9	33
Cr(OH)(BDC)	MIL-53(Cr)	304	1	8.5	34
$Cu_3(BPT)_2$	UMCM-150	298	1	10.2	33

2.4 CO_2 Adsorption Capacity of Basolite C300

Several studies for the adsorption onto Basolite C300 have been reported in the literature. They have applied different temperature and pressure conditions. In general MOFs were found to exhibit lower CO_2 adsorption capacity upon increasing the temperature greater than room temperature. The lower-pressure (<1.2 bar) adsorption capacities for Basolite C300 was collected at ambient temperatures (293-313 K) are presented in Tables 2.3. At these pressures and temperatures, Basolite C300 have shown the maximum adsorption capacity, which clearly indicates its chemical features of the pore surface, and have high efficiency material which bears highly functionalized surface.

For post-combustion CO_2 capture, the pressure of the flue gas (~1 bar) CO_2 adsorption shows the maximum adsorption capacity specifically around 4.5 mmol/g at 303K temperature which would be expected to lead to new material with enhanced performance for post combustion CO_2 capture.

Literature review shows that most of the studies on the MOFs as adsorbents for CO_2 adsorption are performed using pure CO_2 under high pressure and often at room or sub ambient temperature. It has been reported that MOF-117, MIL-101, and IRMOF-1 exhibit exceptional CO_2 storage capacity at high pressure, e.g. 33.5 mmol/g at 40 bar, 40

mmol/g at 50 bar, and 21.7 mmol/g at 35 bar [41,42]. However, their capacities are dramatically reduced under dynamic conditions and sub atmospheric pressure. More recently, in the literature CO_2 adsorption capacity of 8.61 mmol/g at 298 K and low pressure of 1 bar on Mg-MOF-47, 3 mmol/g on CPM-5 and 1.7 mmol/g on MOF-177 at room temperature and low pressure of 1 bar have been reported [43-45].

Table 2.3 CO_2 adsorption capacity of Basolite C300 (HKUST-1) at different conditions

Adsorbent	Pressure (bar)	Temperature (K)	Capacity (mmol/g)	Reference
Basolite C300 (HKUST-1)	1	293	4.5	[35]
	1	298	4.18	[36]
	1	295	4.15	[36]
	1	298	3.45	[37]
	1	295	3.4	[38]
	0.8	298	2.4	[39]
	1	295	1.4	[38]
	1	313	1.4	[40]

To the best of our knowledge, virtually no research work has been conducted to examine the gas adsorption and kinetic properties of MOFs when exposed to a mixture of gases under dynamic conditions. In addition, the number of studies has examined the experimental operating conditions of the breakthrough data [46-50]. Accordingly, it is essential to determine the dynamic adsorption capacity of CO_2 onto MOFs, which can be measured by exposing the adsorbent to a gas stream and detect the breakthrough value corresponding to different feed concentrations.

Chapter-3

EXPERIMENTAL

3.1 Materials

Adsorbent used in this study is Basolite C 300 i.e. copper benzene-1, 3, 5 tricarboxylate or Cu-BTC MOF and it was purchased from M/s Sigma Aldrich and used as received, with molecular weight of 604.87.

N_2, CO_2 and He gases for the sorption study were procured from M/s Sigma Gases and Services, India and were of high purity grade (99.999%).

3.2 Characterization of Basolite C300

3.2.1 Thermogravimetric analysis (TGA)

Basolite C300 was characterized using a TGA model Q500 from TA-Instruments. TGA was used to determine the thermal stability. Approximately 10 mg of sample were heated at a rate of 10°C/min from 23 to 900^{o}C under the nitrogen flow. It is observed that Basolite C300 has good thermal stability upto 150^{o}C. Above 150^{o}C its structure has started collapsing.

3.2.2 X-ray diffraction

X-ray diffraction (XRD) is a versatile, non-destructive technique that reveals detailed information about the chemical composition and crystallographic structure of natural and manufactured materials.

Powder X-ray diffraction study (reported in the literature by Najafi Nobar et al. [30]) of the commercial Basolite C300 sample was obtained using Cu Kα radiation in the 5-45 degrees 2θ range with a scanning speed of 30^{o}/min at operating condition of 40 kV and 30 mA [30]. Cu Kα radiation was bombarded on the dry powder samples to get the diffraction signals. Cu-BTC sample was very fine powder, which helped minimize the effect of preferred orientation on the XRD pattern. The distinct XRD peaks of Basolite C300 are given in Table 3.1.

Table 3.1 XRD patterns of commercial Basolite C300 sample reported in literature [29]

2θ	**d (**Å)
6.7°	1.318
9.5°	0.93
11.65°	0.759
13.5°	0.655
19.3°	0.46
26°	0.342

3.3 Breakthrough Experiment

The adsorption study set-up was designed and got fabricated and assembled by Chemito Technologies Pvt. Ltd., Mumbai shown in Fig. 3.1. Adsorption study set up was followed by Gas Chromatograph shown in Fig. 3.2, purchased from Agilent Technologies, India, for the quantitative analysis of the gas mixtures. Measurements of sorption kinetics in gas phase were carried out in a fixed bed adsorption reactor. The experimental set up consisted of (1) a stainless steel fixed-bed adsorption column (ID = 9.0mm, L = 300mm) placed in an oven 2) a bypass line for measuring the feed concentration, (3) flow meters/controllers (MFC) to control the flow-rates of the inlet gases, (4) a gas mixture; the inlet gases mix thoroughly before flowing through the adsorbent bed, (5) and an online gas chromatograph (GC 7890A, Agilent Technologies, US) equipped with a TCD detector and a capillary column to measure the CO_2 concentration. Helium gas was selected as the carrier gas. Schematic diagram of the adsorption set up is shown in Fig. 3.3 for better understanding.

Fig. 3.1 Adsorption set up

Fig 3.2 Gas chromatograph apparatus

The experiments were performed as follows: 1g of powder Basolite C300 was loaded into the reactor along with the glass beads and fixed between glass wool i.e. on both top and bottom sides of the reactor. Glass beads are used to reduce the dead volume in the column. For the adsorption tests, the Basolite C300 adsorbent was activated under nitrogen (N_2 flow rate = 50 ml/min) at 423K for 3 hours to remove all the moisture and adsorbed gases. After that, the temperature was decreased and CO_2 in N_2 was introduced at a flow rate of 8 ml/min resulting in a gas mixture with CO_2 content of 10% by volume. Similar experiments were performed at different temperatures and feed concentrations shown in Table 3.2. Reproducibility of the results was confirmed by repeating several of these runs.

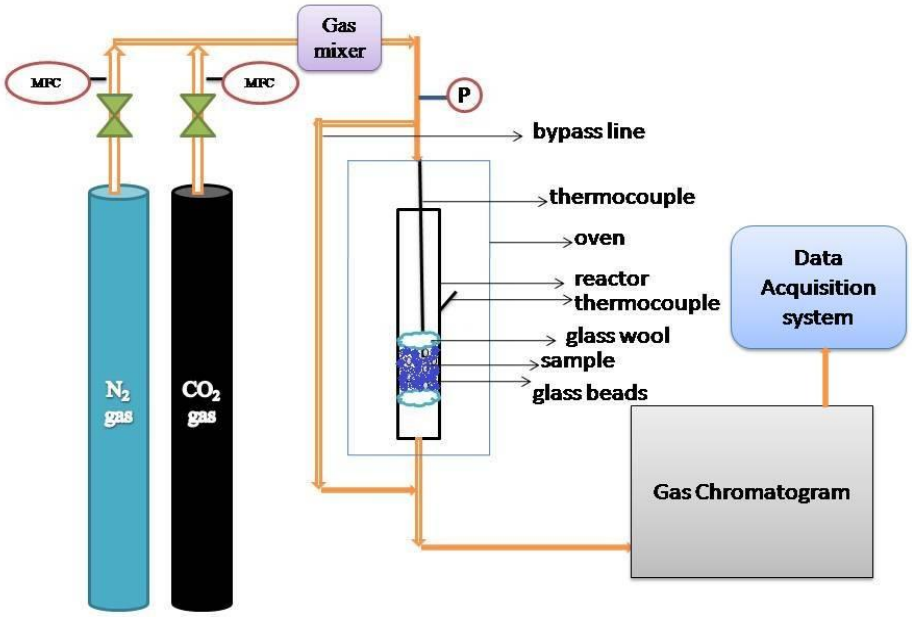

Fig. 3.3 Schematic diagram of adsorption set up

Table 3.2 Experimental conditions for breakthrough study on Basolite C300

CO_2 Concentration (%)	Adsorption Temperature (^oC)
10	30
10	50
10	75
10	100
5	30
7.5	30
12.5	30

3.3.1 Capacity calculation

The activity of the adsorbent towards CO_2 was defined by breakthrough curves. The dynamic adsorption capacity is calculated in each case by dividing the total mass of gas adsorbed before breakthrough by the mass of adsorbent. Also, plot of the C/C_o vs. time is integrated to obtain the area under the curve. The adsorption capacity was calculated by the following equation

$$q_t = \frac{Q}{mV_m} \int_0^t (C_o - C)\, dt \qquad \text{.....(3.1)}$$

where q_t is the CO_2 adsorption capacity in mmol/g; m is the mass of the adsorbent used in experiment, g; Q is the gas flow rate in ml/min and t is time in minutes; C_o is the initial feed concentration of CO_2; C is the outlet concentration of CO_2 at time t [51]; V_m is the molar concentration of the gas. By plotting the breakthrough curve i.e. C/C_o vs. time adsorption capacity is calculated.

3.3.2 Selectivity

The selectivity of CO_2 over species *i* in the binary mixture of CO_2 and species *i* is determined using the following equation:

$$S_{CO_2} = \frac{\frac{x_{CO_2}}{x_i}}{\frac{y_{N_2}}{y_i}} \qquad \text{…….(3.2)}$$

where *x* and *y* refer to the molar composition of the adsorbed phase and the gas phase, respectively.

3.4 Adsorption Kinetics

Adsorption kinetics gives the adsorbate adsorption rate. To study the adsorption on solid adsorbent, two models were adopted i.e. pseudo first and pseudo second order model. Adsorption of carbon dioxide on the Basolite C300 was performed at four different temperatures (303 K, 323 K, 348 K, and 373 K).

3.4.1. Pseudo first order equation (Lagergren model)

The Lagergren model, assumes a first order adsorption kinetics which can be represented by the equation:

$$\log(q_e - q_t) = \log q_e - \frac{k_1 t}{2}.303 \qquad \text{…….. (3.3)}$$

Where qe and q_t are adsorption capacity at equilibrium and at time t, respectively (mmol/g), k_1 is the rate constant of pseudo first order adsorption (min^{-1}) [52,53].

3.4.2. Pseudo second order equation

The pseudo second-order adsorption kinetic rate equation is expressed as:

$$\frac{t}{q_t} = \frac{1}{k_2 q_e^2} + \frac{t}{q_e} \qquad \text{…….. (3.4)}$$

where k_2 (g/mmol.min) is the rate constant and q_e and q_t (mmol/g) are adsorption capacity at equilibrium and at time t (min), respectively [34,54].

3.4.3. Validity of kinetic models

The sum of error squares (SSE, %) is one method, which has been used in literature to test the validity of each model that has been used. The sum of error squares is given as [57].

$$SSE = \sqrt{\sum \frac{[(q]_{e,expt} - q_{e,cal})^2}{N}} \qquad \text{....…... (3.5)}$$

Where $q_{e,exp}$ and $q_{e,cal}$ refer to the experimental and calculated CO_2 uptake, N is the number of data points.

3.5 Adsorption Isotherms

Equilibrium studies that give the capacity of the adsorbent and the equilibrium relationships between adsorbent and adsorbate are described by adsorption isotherms, which are usually the ratio between the quantity adsorbed and the remaining in solution at fixed temperature at equilibrium. Here, Equilibrium data were analyzed using the Langmuir and Freundlich isotherm models. These isotherms are the two most commonly used equilibrium relations [56].

3.5.1 Langmuir isotherm

The formation of a monolayer adsorbate on the surface of the adsorbent, and after that no further adsorption takes place [56]. The model assumes uniform energies of adsorption onto the surface and no exploration of adsorbate in the plane of the surface. Based upon these assumptions, Langmuir represented the following equation:

$$q_e = \frac{q_o K_l C_e}{1 + K_l C_e} \qquad \text{…….(3.6)}$$

Where:

C_e = the equilibrium concentration of adsorbate (mg/L)

q_e = the amount of carbon dioxide adsorbed per gram of the adsorbent at equilibrium (mg/g)

q_o = maximum monolayer coverage capacity (mg/g)

K_l = Langmuir isotherm constant (L/mg)

3.5.2 Freundlich Adsorption Isotherm

It is commonly used to describe the adsorption characteristics for the heterogeneous surface [57]. The data often fit the empirical equation proposed by Freundlich.

$$q_e = K_f C_e^{\frac{1}{n}} \qquad \text{…….(3.7)}$$

where K_f and n are Freundlich constants related to adsorption capacity and adsorption intensity of adsorbents, respectively. The value of n falling in the range of 1–10 indicates favorable adsorption. Also, C_e is the equilibrium concentration (mg/L), q_e the amount of the adsorbent adsorbed (mmol/g).

Chapter-4

RESULTS AND DISCUSSION

4.1 Characterization

4.1.1 Thermogravimetric analysis

TGA was done at atmospheric pressure under the pure nitrogen atmosphere upto the temperature of 900^{o}C. The weight loss of the Basolite C300 was seen in two stages; approximately 34% of the weight loss upto 100^{o}C is because of the water present in the sample and another 36% weight loss is upto 400^{o}C is because of the breakage of the structure at higher temperature. It can be clearly seen that sample is stable upto 300^{o}C. Therefore, it should be activated below 300^{o}C prior to adsorption and breakthrough measurements. Similar results have been reported by Najafi Nobar et al. [29], they have carried out the thermal stability test under the helium flow from 30^{o}C to 400°C. The weight loss pattern of the sample is very similar i.e. 40% weight loss upto 100°C and 32% weight loss upto 300°C, which shows that the sample is stable upto 300°C.

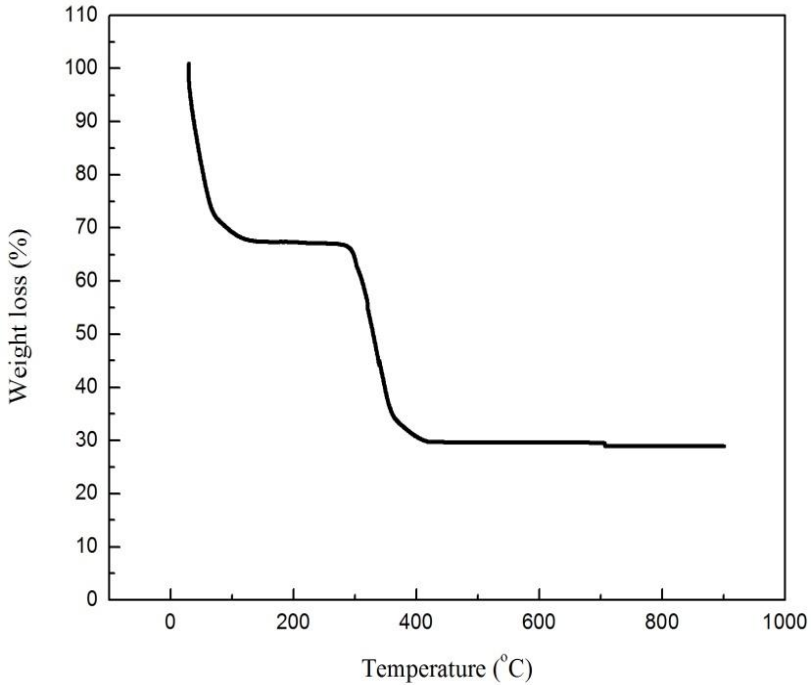

Fig. 4.1 TGA curve of the Basolite C300

4.2 CO_2 adsorption study

4.2.1 Effect of adsorption temperature

The effects of adsorption temperature on Basolite C300 were evaluated by analyzing the breakthrough curves at different temperatures. On increasing the temperature, the additional energy increases the internal energy of the molecules and helps the molecules to escape (desorbs) faster from the surface and equilibrium comes faster [23]. It can be seen in the Fig 4.2 that the breakthrough time of CO_2 decreased from 17 min to 10 min as the temperature was increased from 303K to 373K. Therefore, as the temperature increases, it gets saturated faster. The breakthrough for N_2 shows a hump. This is the typical nature of a breakthrough curve where competitive adsorption is taking place. Initially, N_2 being in higher concentration occupies more sites. With time, kinetic selectivity for CO_2 plays a role, and the adsorbed N_2 is displaced making space for CO_2 [60]. Thus, the outlet concentration of N_2 shows a hump of concentration over that in the feed. Also, nitrogen gas attains the equilibrium faster as compared to carbon dioxide gas, which clearly indicates the higher selectivity of CO_2 over N_2.

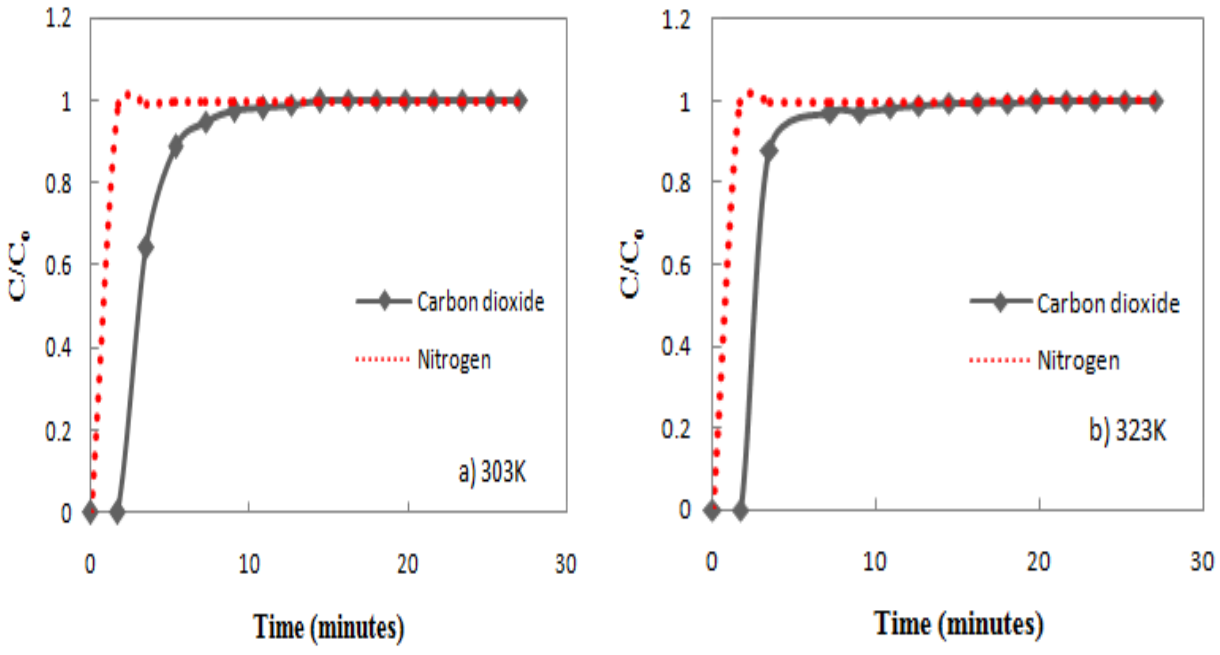

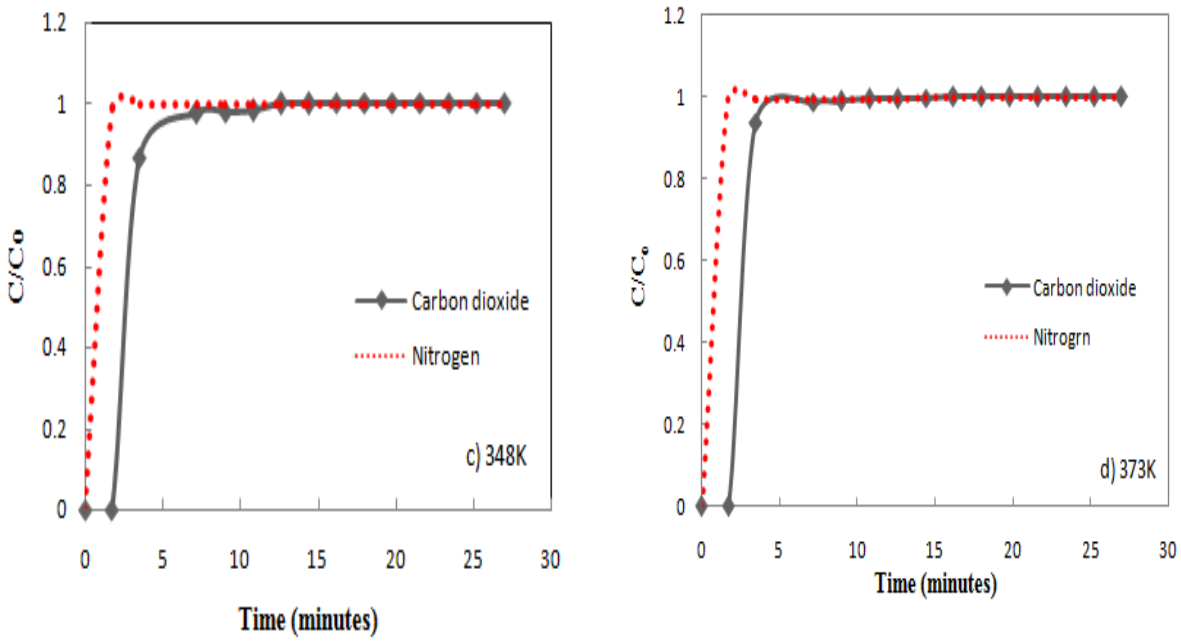

Fig. 4.2 Breakthrough curves of Basolite C300 at different adsorption temperatures at 10% CO_2 feed concentration (90% N_2)

Adsorption capacity of Basolite C300 was calculated by using equation 3.1 from Chapter 3 from the above breakthrough curves, obtained values are given in the Table 4.1. The maximum adsorption is observed at 303K i.e. 1.45 mmol/g. Increase in temperature may cause the decrease in the adsorptive forces between the carbon dioxide and the active sites on the adsorbent surface, which leads to the decrease in the adsorption capacity. Adsorption capacity decreased from 1.45 mmol/g to 1.13 mmol/g with increase in the temperature from 303 K to 373 K.

Table 4.1 Adsorption capacity of Basolite C300 at different temperatures at 10% CO_2 concentration

Temperature (K)	303	323	348	373
$q_{e,exp,CO2}$ (mmol/g)	1.45	1.31	1.26	1.17
$q_{e,exp,N2}$ (mmol/g)	0.45	0.39	0.35	0.30

CO_2/N_2 selectivity on Basolite C300 at different temperatures is shown in Table 4.2. These values were calculated from Ideal Adsorbed Solution Theory (IAST). Basolite C300 shows increasing CO_2/N_2 selectivity with increase in temperature. This selectivity behavior is explained by Mishra et al. [59]. At lower temperatures, when the structure of the adsorbent is not rigid, a host of factors governs the adsorption characteristics of a gas mixture. In any case, for separation of CO_2 from industrial flue gases, selectivity values at higher temperatures will be more relevant [60].

Basolite C300 selectivities are considerably higher than the experimental CO_2/N_2 selectivities reported for zeolite and carbon adsorbents under similar conditions: zeolite 13X (18) [61], activated carbon (15) [62].

Table 4.2 Adsorption selectivity of CO_2 vs. N_2 onto Basolite C300 at different temperatures

Temperature (K)	303	323	348	373
Selectivity	29.02	30.26	32.43	35.10

4.2.2 Effect of feed concentration

The effect of the inlet CO_2 concentration on the breakthrough curve was studied at four different CO_2 concentrations of 5%, 7.5%, 10%, and 12.5% at 303K as shown in Fig. 4.3. As the inlet concentration of CO_2 was increased from 5% to 12.5%, the breakthrough time decreased from 16.2 to 10.8 minutes. The bed gets saturated faster at higher concentration of CO_2. As seen, N_2 appears in the column immediately after the process has started, indicating a very small adsorption capacity for N_2, if any [63] but it gets saturated faster as compared to CO_2, which clearly shows the higher selectivity of CO_2 over N_2 shown in the Table 4.3. CO_2/N_2 selectivity in Basolite C300 at different feed concentrations was calculated using equation 3.2 from Chapter 3. The selectivity increases as y_{N2} approaches unity [64]. Here, y_{N2} increases from 87.5% to 95%, which causes an increase in y_{N2}, therefore selectivity of CO_2/N_2 increases in the range of 19.8 to 68.6.

Table 4.3 Adsorption selectivity of Basolite C300 at different concentrations

CO_2 Concentration (%)	5	7.5	10	12.5
Selectivity	68.6	39.38	28.3	19.8

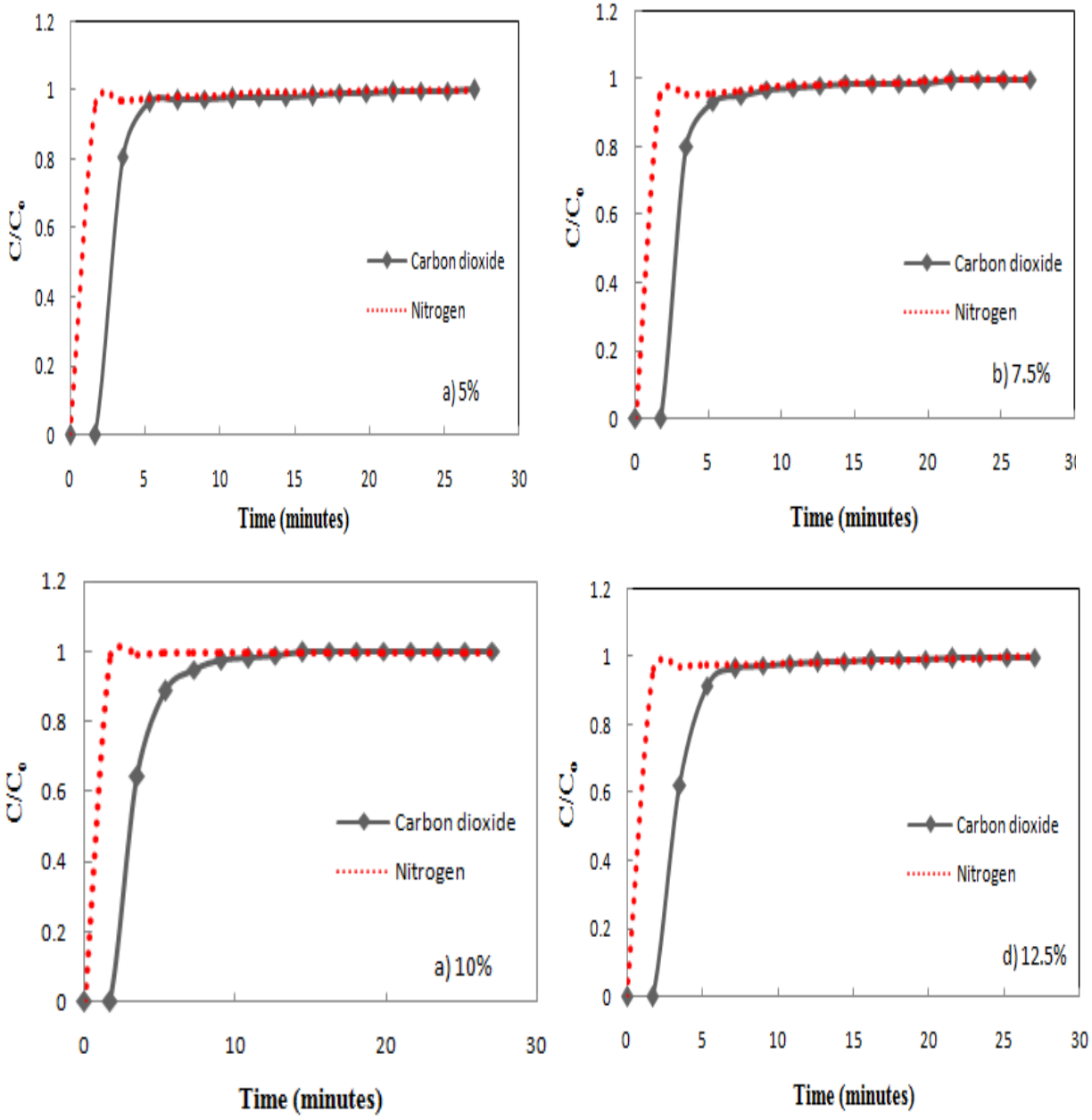

Fig. 4.3 Breakthrough curves of Basolite C300 at different feed CO_2 concentrations at 303K

The adsorption capacities (q_e) at different inlet concentrations of CO_2 obtained from Fig. 4.3 are

listed in Table 4.4. With the increase of CO_2 concentration from 5% to 12.5% adsorption capacity (mmol/g) increased from 1.30 to 1.47 mmol/g because at higher CO_2 concentration driving force is larger and more time it will take to get saturated. Also, at higher concentration, the availability of the molecules for the adsorption sites is more, which leads to higher uptake of CO_2 at higher concentration even though the breakthrough time is shorter than the breakthrough time of lower concentrations. Thus, the equilibrium is attained faster for higher CO_2 concentration.

Table 4.4 Adsorption capacity of Basolite C300 at different concentrations at 303K

CO_2 Concentration (%)	5	7.5	10	12.5
$q_{e,exp,CO2}$ (mmol/g)	1.30	1.34	1.45	1.47
$q_{e,exp,N2}$ (mmol/g)	0.36	0.40	0.46	0.52

To evaluate the efficiency of the Basolite C300 adsorbent for CO_2 capture, the results obtained in this work are compared with those reported in the literature for other similar adsorbents. CO_2 adsorption data of different adsorbents including Basolite C300 (this work) are summarized in Table 4.5.

Table 4.5 Comparison of CO_2 adsorption capacity of Basolite C300 with some other porous materials reported in the literature

Material	Temperature (K)	Adsorption capacity (mmol/g)	Reference
Cu-BTC	303	1.45	This work
Amino-MIL-53	303	0.84	65
ZIF-78	298	0.32	66
MOF-177	298	0.81	31

According to these data, Basolite C300 adsorbent shows a higher breakthrough storage capacity for CO_2 (i.e. 1.45 mmol/g) compared with other reported materials at the similar experimental conditions. Due to the presence of copper metal i.e. Cu^{2+} sites interact more strongly with CO_2 due to high charge density. Copper has high electrostatic interaction with carbon dioxide compared to other adsorbents. Therefore, it can be concluded that the

tested Basolite C300 adsorbent represents a very promising candidate for CO_2 capturing compared to other solid porous adsorbents including Amino MIL-53, ZIF-78 and MOF-177.

4.2.3 Cyclic adsorption/desorption behavior of Basolite C300

The key challenge regarding carbon dioxide capture technologies is that the capture materials used should be regenerable. In order to examine the regeneration of the Basolite C300 adsorbent and its efficiency, it was tested under four repeated adsorption-desorption cycles at 303K and 423K as shown in Fig 4.4.

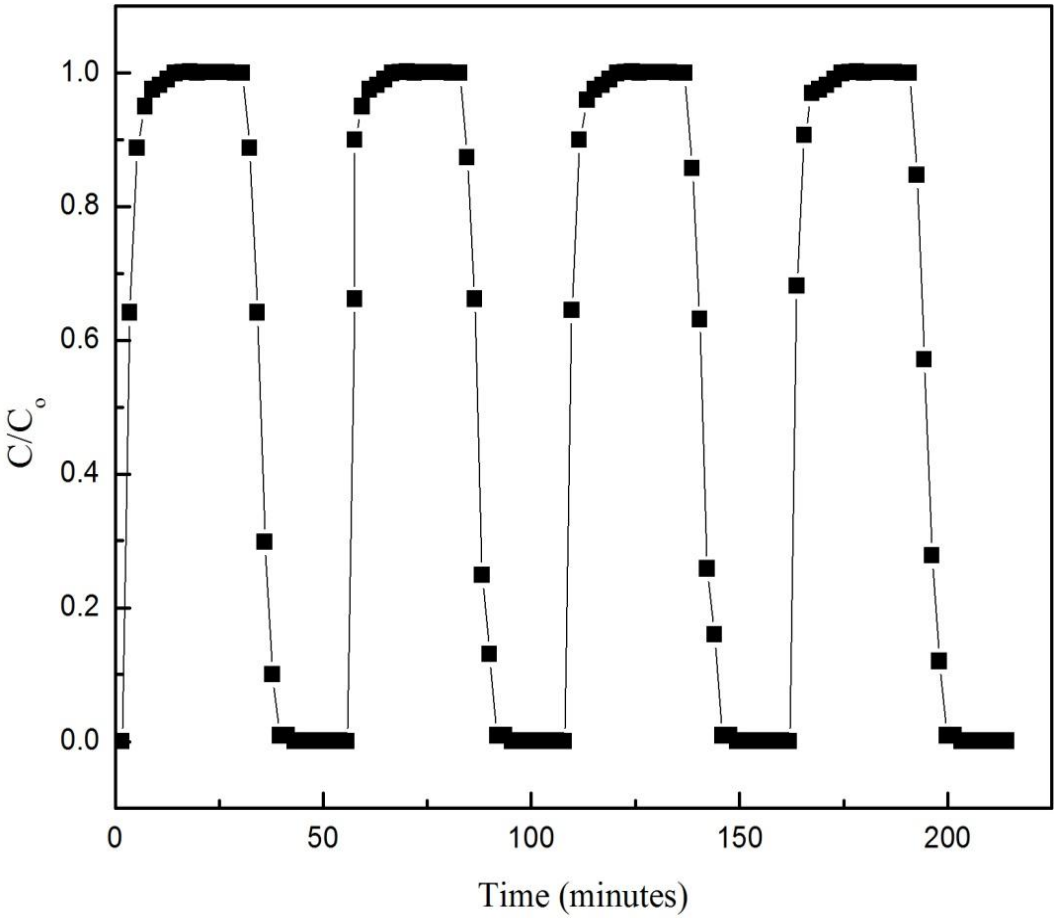

Fig. 4.4 CO_2 adsorption-desorption concentration profile of Basolite C300 at 303K

For temperature swing adsorption (TSA) regeneration method, desorption efficiency increases with the increasing temperature. Desorption was done under the pure nitrogen by increasing the fixed bed temperature to 423K.

According to the experimental data presented in Figure 4.4, it can be seen that the adsorption behavior of the regenerated Basolite C300 is the same as the fresh sample. There is an instantaneous fall of C/C_o values, which clearly indicates the easy removal of CO_2 from the surface. In each cycle of adsorption and desorption Basolite C300 shows its capability to regain its property again, which shows its good reusability. This means the Basolite C300 is fully recovered at the applied regeneration conditions.

4.3 Kinetics study

In order to understand the kinetics of adsorption of carbon dioxide onto Basolite C300 as an adsorbent, pseudo first and pseudo second order models were applied. The equations (3.3) and (3.4), shown in the Chapter 3, were fitted to the experimental data using a non linear regression method to get the kinetic parameters. It can be seen in Fig 4.5 that pseudo second order curve is closer to the experimental data curve.

.

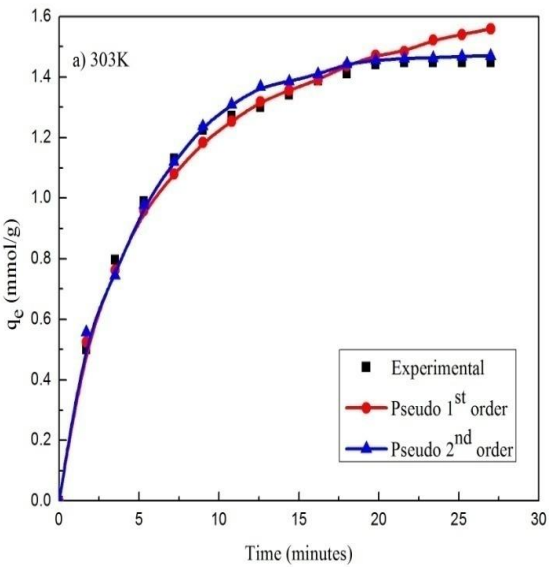

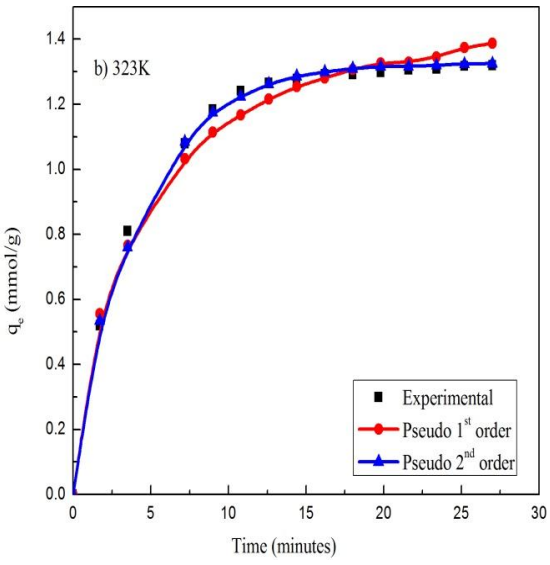

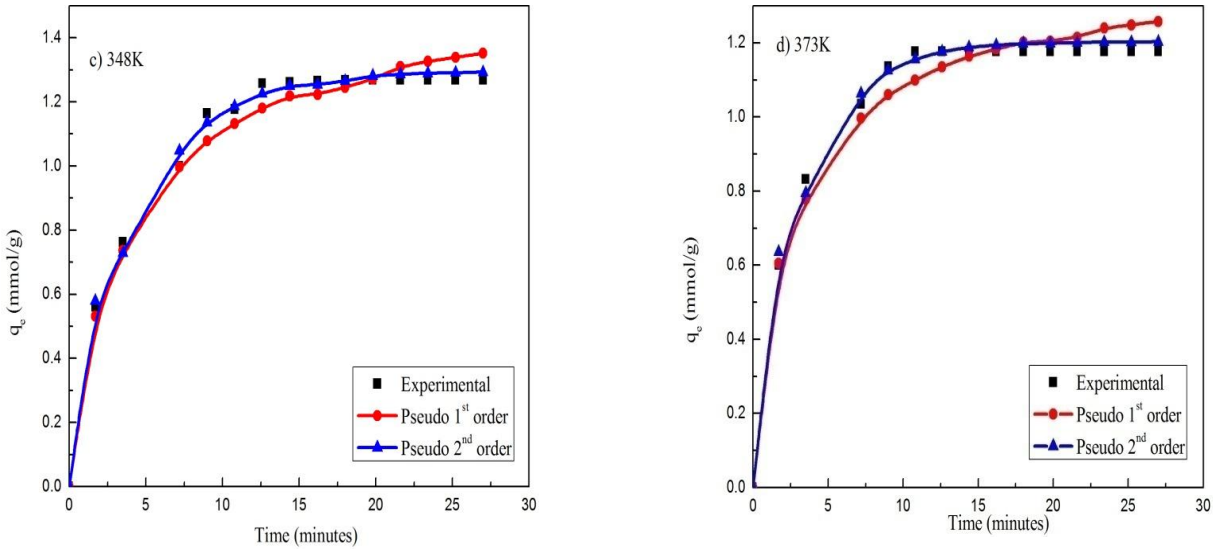

Fig. 4.5 Pseudo First order, pseudo second order and experimental kinetic model plot at different temperature (a) 303 K, (b) 323 K, (c) 348 K and (d) 373 K

The best fit values of $q_{e,cal}$, k_1 and k_2 along with the correlation coefficient are given in Table 4.6. The values of calculated adsorption capacity, $q_{e,cal}$ obtained from the pseudo second order kinetic model are very close to experimental adsorption capacity, $q_{e,exp}$. The calculated correlation coefficients R^2 are also closer to unity i.e. 0.99 for pseudo second order kinetics. Therefore, the adsorption can be approximated more appropriately by pseudo second order as compared to the pseudo first order kinetic model for the adsorption of carbon dioxide on Basolite C300.

Table 4.6 Pseudo-first-order and pseudo-second-order models rate constants calculated from experimental data at 10% concentration of CO_2

Kinetic models	Temperatures (K)			
	303	323	348	373
$q_{e,exp}$ (mmol/g)	1.45	1.31	1.26	1.17
Pseudo first order				
$q_{e,cal}$ (mmol/g)	1.49	1.38	1.36	1.25
k_1 (1/min)	0.35	0.84	1.01	0.75
R^2	0.99	0.98	0.98	0.96
SSE (%)	0.022	0.035	0.041	0.072
Pseudo second order				
$q_{e,cal}$ (mmol/g)	1.44	1.32	1.29	1.20
k_2 (g/mmol.min)	0.25	1.28	1.64	0.861
R^2	0.99	0.99	0.99	0.99
SSE (%)	0.038	0.012	0.021	0.042

4.4 Isotherms

The Langmuir and Freundlich isotherms were fitted as shown in Fig. 4.6. It is demonstrated that the agreement between the Langmuir isotherm and the experimental data is high. The red color line represents the Langmuir lines, which is best, fitted on the experimental data; it has good correlation coefficient (R^2) value of 0.998.

The values of the isotherm constants are calculated and given in Table 4.7. It can be seen that the regression correlation coefficient (R^2) of the Langmuir equation 0.998 is higher than that for the Freundlich equation (R^2 = 0.995), which clearly shows that the adsorption isotherm data are well fitted by the Langmuir isotherm. The results indicated that the maximum CO_2 adsorption capacity (q_o) of Basolite C300 was 2.65 mmol/g.

The Langmuir isotherm was applied for the evaluation of maximum adsorption capacity corresponding to complete monolayer coverage on the adsorbents as the CO_2 adsorption onto Basolite C300 could be a monolayer adsorption onto a homogeneous surface of the adsorbent.

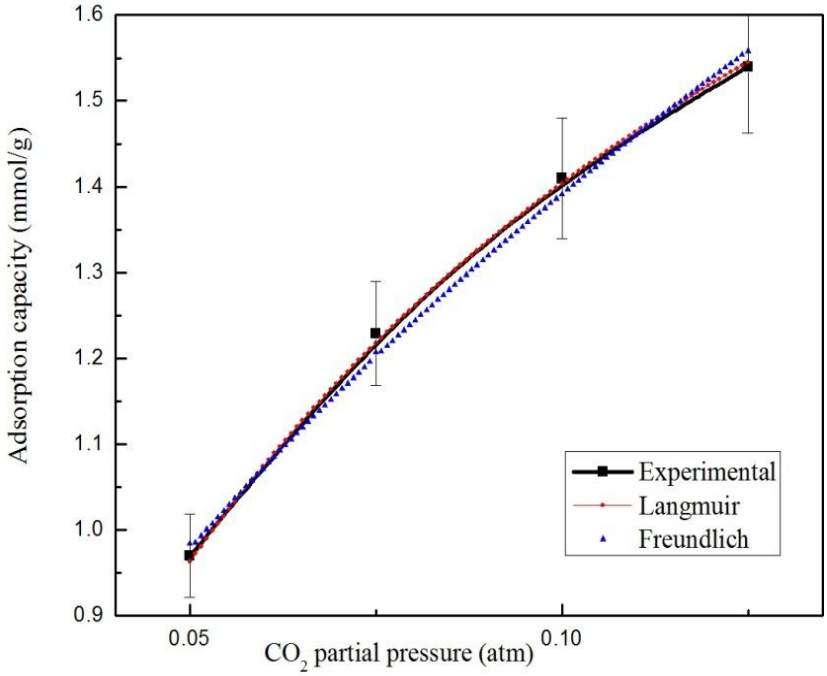

Fig. 4.6 Experimental and model predicted CO_2 adsorption isotherm of Basolite C300 at 303K

Freundlich adsorption isotherm describes a monolayer adsorption onto a heterogeneous surface of the adsorbent. In Freundlich isotherm value of 'n' indicates the degree of nonlinearity between adsorbate concentration and adsorption as follows: if n=1, then adsorption is linear; if n <1, then adsorption is a chemical process; if n>1, then adsorption is a physical process [57]. The value of n in Freundlich equation was found to be 1.92 as shown in Table 4.7. The situation is most common and may be due to a distribution of surface sites or any factor that causes a decrease in adsorbent-adsorbate interaction with increasing surface sites. In the present study, since it lies between 1 and 10, it indicates the physical adsorption.

Table 4.7 Isotherm model parameters

Isotherm model		Kinetic parameters
Freundlich	$q_e = K_f C_e^{\frac{1}{n}}$	K_f = 4.625, n = 1.92, R^2 = 0.995
Langmuir	$q_e = \frac{q_o K_l C_e}{1 + K_l C_e}$	K_l = 11.36, q_o = 2.65, R^2 =0.998

Chapter-5

CONCLUSIONS

The research of this dissertation is focused on the adsorption of carbon dioxide using one of the metal organic frameworks. Here, Basolite C300 is used as an adsorbent. Basolite C300 was tested for dynamic CO_2 adsorption using a laboratory scale reactor column. Based on the experimental work, following conclusions are made:

1) Breakthrough study reveals that the adsorbent performed better at lower temperature and higher concentration.
2) Pseudo second order kinetic model fitted better than the pseudo first order. The maximum adsorption capacity of Basolite C300 at 303K is 1.45 mmol/g.
3) Experimental data followed Langmuir isotherm better than Freundlich isotherm.
4) Basolite C300 is stable upto 573K.

The results show that Basolite C300 has the potential to be developed into an efficient adsorbent for the removal of carbon dioxide from flue gas.

REFERENCES

[1] N. Mac Dowell, N. Florinn, A. Buchard, J. Hallet, A. Galindo, G. Jackson, C. Adjiman, C. Williams, N. Shah, P. Fennell, An overview of CO_2 capture technologies, Phys. Chem. Chem. Phys., 12 (2010) 1–29.

[2] M. Kanniche, R. G. Bonnivard, P. Jaud, J. V. Marcos, J. M. Amann, C. Bouallou, Precombustion, post combustion and oxy combustion in thermal power plant for CO_2 capture, Appl. Therm. Eng., 30 (2010) 53–62.

[3] A. S. Bhown, B. C. Freeman, Analysis and status of post combustion carbon dioxide capture technologies, Environ. Sci. Technol., 45 (2011) 8624–8632.

[4] F. Raganati, V. Gargiulo, P. Ammendola, M. Alfe, R. Chirone, CO_2 capture performance of HKUST-1 in a sound assisted fluidized bed, Chem. Eng. J., 239 (2014) 75–86.

[5] S. Choi, J. H. Drese, C. W. Jones, Adsorbent materials for carbon dioxide capture from large anthropogenic point sources, ChemSusChem, 2 (2009) 796−854.

[6] D. M. D'Alessandro, B. Smit, J. R. Long, Carbon dioxide capture: prospects for new materials, Angew. Chem. Int. Ed. 49 (2010) 6058−6082.

[7] S. Sjostrom, H. Krutka, Evaluation of solid sorbents as a retrofit technology for CO_2 capture, Fuel, 89 (2010) 1298−1306.

[8] R. Vaidhyanathan, S. S. Iremonger, G. K. H. Shimizu, P. G. Boyd, S. Alavi, T. K. Woo, Direct observation and quantification of CO_2 binding within an amine-functionalized nanoporous solid, Sci., 330 (2010) 650−653.

[9] A. Samanta, A. Zhao, G. K. H. Shimizu, P. Sarkar, R. Gupta, Post combustion CO_2 capture using solid sorbents: A Review, Ind. Eng. Chem. Res., 51 (2011) 1438−1463.

[10] K. Sumida, D.L. Rogow, J.A. Mason, T.M. McDonald, E.D. Bloch, Z.R. Herm, T.H. Bae, J. R. Long, Carbon dioxide capture in metal-organic frameworks, Chem. Rev., 112 (2012) 724–781.

[11] J. R. Li, Y. Mab, M.C. McCarthy, J. Sculleya, J. Yub, Carbon dioxide capture-related gas adsorption and separation in metal-organic frameworks, Coord. Chem. Rev., 255 (2011) 1791–1823.

[12] H. Wu, W. Zhou, T. Yildirim, High-capacity methane storage in metal−organic frameworks M_2(dhtp): the important role of open metal sites, J. Am. Chem. Soc., 131 (2009) 4995-5000.

[13] K. Munusamy, G. Sethia, D.V. Patil, P.B.S. Rallapalli, R.S. Somani, H.C. Bajaj, Sorption of carbon dioxide, methane, nitrogen and carbon monoxide on MIL-101(Cr): volumetric measurements and dynamic adsorption studies, J. Chem. Eng. 195–196 (2012) 359–368.

[14] R. K Pachauri, A. Reisinger, Intergovt. Panel on Clim. Change, (2013).

[15] H. Furukawa, N. Ko, Y. B. Go, N. Aratani, S. B. Choi, E. Choi, A. O. Yazaydin, R.Q. Snurr, M. O'Keeffe, J. Kim, O.M. Yaghi, Ultra-high porosity in metal-organic frameworks, Sci. 329, 424-428 (2010).

[16] D. Aaron, C. Tsouris, Separation of CO_2 from Flue Gas: A Review, Separ. Sci. Technol., 40 (2005) 321-348.

[17] A. Sayari, Y. Belmabkhout, R. Serna-Guerrero, Flue gas treatment via CO_2 adsorption, Chem. Eng. J., 171(2011) 760–774.

[18] S. Kenji, D. L. Rogow, J. A. Mason, T. M. McDonald, E. D. Bloch, Z. R. Herm, T. H. Bae, J. R. Long, Carbon dioxide capture in metal organic frameworks, Chem. Rev., 112 (2012) 724–781.

[19] J. Rother, T. Fieback, Multicomponent adsorption measurements on activated carbon, zeolite molecular sieve and metal organic framework, Adsorption, 19 (2013) 1065–1074.

[20] J. R. Li, R. J. Kuppler, H. C. Zhou, Selective gas adsorption and separation in metal–organic frameworks, Chem. Soc. Rev., 38 (2009) 1477-1504.

[21] R. E. Morris, P. S. Wheatley, Gas storage in nanoporous materials, Angew. Chem. Int. Ed., 47 (2008) 4966-4981.

[22] G. Ferey, Hybrid porous solids: past, present, future, Chem. Soc. Rev., 37 (2008) 191-214.

[23] N. A. Rashidi, S. Yusup, H. L. Lam, Kinetic studies on carbon dioxide capture using activated carbon, Chem. Eng. Trans., 35 (2013) 361-366.

[24] S. S. Y. Chui, S. M. F. Lo, J. P. H. Charmant, A. G. Orpen, I. D. Williams, A Chemically functionalizable nanoporous material $[Cu_3(TMA)_2(H_2O)_3]_n$, Sci., 283 (1999) 1148–1150.

[25] C. Prestipino, L. Regli, J. G. Vitillo, F. Bonino, A. Damin, C. Lamberti, Local structure of framework Cu(II) in HKUST-1 metallorganic framework: spectroscopic characterization upon activation and interaction with adsorbates, Chem. Mater., 18 (2006) 1337–1346.

[26] S. T. Meek, J. A. Greathouse, M. D. Allendorf, Metal organic frameworks: A rapidly growing class of versatile nanoporous materials, Adv. Mater., 23 (2011) 249–267.

[27] S. Bordiga, L. Regli, F. Bonino, E. Groppo, C. Lamberti, B. Xiao, P. S. Wheatley, R. E. Morris, A. Zecchina, Adsorption properties of HKUST-1 toward hydrogen and other small molecules monitored by IR, Phys. Chem. Chem. Phys., 9 (2007) 2676–2685.

[28] R. J. Karra, S. K. Walton, Effect of open metal sites on adsorption of polar and nonpolar molecules in metal organic framework Cu-BTC, Langmuir, 24 (2008) 8620-8626.

[29] S. Najafi Nobar, S. Farooq, Experimental and modeling study of adsorption and diffusion of gases in Cu-BTC, Chem. Eng. Sci., 84 (2012) 801-813.

[30] K. Schlichte, T. Kratzke, S. Kaskel, Improved synthesis, thermal stability and catalytic properties of metal organic framework compound $Cu_3(BTC)_2$, Micropor. Mesopor. Mat., 73 (2004) 81-88.

[31] J. Mason, K. Sumida, Z. Herm, R. Krishna, J. Long, Evaluating metal-organic frameworks for post combustion carbon dioxide capture via temperature swing adsorption, Energ. Environ. Sci., 4 (2011) 3030-40.

[32] Z. Bao, L. Yu, Q. Ren, X. Lu, S. Deng, Adsorption of CO_2 and CH_4 on a magnesium based metal organic framework, J. Colloid Interf. Sci., 353 (2011) 549-56.

[33] A. Yazaydin, R. Q. Snurr, T. H. Park, K. Koh, J. Liu, M. D. Levan et al., Screening of metal organic frameworks for carbon dioxide capture from flue gas using a combined experimental and modeling approach, J. Am. Chem. Soc., 131 (2009) 18198-9.

[34] P. L. Llewelly, S. Bourrelly, C. Serr, Y. Filinchuk, G. Ferey, How hydration drastically improves adsorption selectivity for CO_2 over CH_4 in the flexible chromium terephthalate MIL-53, Angew. Chem. Int. Ed., 45 (2006) 7751-4.

[35] P. Aprea, D. Caputo, N. Gargiulo, F. Iucolano, F. J. Pepe, Modeling carbon dioxide adsorption on microporous substrates: comparison between Cu-BTC metal organic framework and 13X zeolitic molecular sieve, Chem. Eng. Data, 55 (2010) 3655-3661.

[36] A. O. Yazaydin, A. I. Benin,S. A. Faheem, P. Jakubczak, J. L. Low, R. R. Willis, R. Q. Snurr, Enhanced CO_2 adsorption in metal organic frameworks via occupation of open-metal sites by coordinated water molecules, Chem. Mater., 21 (2009) 1425-1430.

[37] A. R. Millward, O. M. Yaghi, Metal organic frameworks with exceptionally high capacity for storage of carbon dioxide at room temperature, J. Am. Chem. Soc., 127 (2005) 17998–17999.

[38] P. Chowdhury, C. Bikkina, D. Meister, F. Dreisbach, S. Gumma, Comparison of adsorption isotherms on Cu-BTC metal organic frameworks synthesized from different routes, Micropor. Mesopor. Mat., 117 (2009) 406-413.

[39] J. Liu, Y. Wang, P. Jakubczak, R. R. Willis, M. D. Levan, CO_2/H_2O adsorption equilibrium and rates on metal organic frameworks: HKUST-1 and Ni/DOBDC, Langmuir, 26 (2010) 14301–14307.

[40] D. Farrusseng, C. Daniel, C. Gaudillere, U. Ravon, Y. Schuurman, C. Mirodatos, D. Dubbeldam, H. Frost, R. Q. Snurr, Heats of adsorption for seven gases in three metal organic frameworks: systematic comparison of experiment and simulation, Langmuir, 25 (2009) 7383-7388.

[41] C. Ferey, C. Mellot-Draznieks, C. Serre, F. Millange, J. Dutour, S. Surble, I. Margiolaki, Chromium terephthalate based solid with unusually large pore volumes and surface area, Sci., 309 (2005) 2040−2042.

[42] P. L. Llewellyn, S. Bourrelly, C. Serre, A. Vimont, M. Daturi, L. Hamon, G. D. Weireld, J. Chang, D. Hong, Y. K. Hwang, S. H. Jhung, G. Férey, High uptakes of CO_2 and CH_4 in mesoporous metal-organic frameworks MIL-100 and MIL-101, Langmuir, 24 (2008) 7245−7250.

[43] D. Britt, D. Tranchemontagne, O. M. Yaghi, Metal-organic frameworks with high capacity and selectivity for harmful gases, Proc. Natl. Acad. Sci. U. S. A., 105 (2008) 11623–11627.

[44] R. Sabouni, H. Kazemian, S. Rohani, Mathematical modeling and experimental breakthrough curves of carbon dioxide adsorption on metal organic framework CPM-5, Environ. Sci. Technol., 47 (2013) 9372-80.

[45] D. Saha, Z. Bao, F. Jia, S. Deng, Adsorption of CO_2, CH_4, N_2O, and N_2 on MOF-5, MOF-177, and zeolite 5A, Environ. Sci. Technol., 44 (2010) 1820−1826.

[46] D. Britt, D. Tranchemontagne, O. M. Yaghi, Metal organic frameworks with high capacity and selectivity for harmful gases, Proc. Natl. Acad. Sci. U. S. A., 105 (2008) 11623−11627.

[47] J. Liu, J. Tian, P. K. Thallapally, B. P. McGrail, Selective CO_2 capture from flue gas using metal organic frameworks—a fixed bed study, J. Phys. Chem. C, 116 (2012) 9575−9581.

[48] D. Britt, H. Furukawa, B. Wang, T. G. Glover, O. M. Yaghi, Highly efficient separation of carbon dioxide by a metal-organic framework replete with open metal sites, Proc. Natl. Acad. Sci. U. S. A., 106 (2009) 20637−20640.

[49] N. R. Stuckert, R. T. Yang, CO_2 capture from the atmosphere and simultaneous concentration using zeolites and amine grafted SBA-15, Environ. Sci. Technol., 45 (2011) 10257−10264.

[50] Y. Liu, Q. Ye, M. Shen, J. Shi, J. Chen, H. Pan, Y. Shi, Carbon dioxide capture by functionalized solid amine sorbents with simulated flue gas conditions, Environ. Sci. Technol., 45 (2011) 5710−5716.

[51] A. A. Ahmad, B.H. Hameed, Fixed bed adsorption of reactive azo dye onto granular activated carbon prepared from waste, J. Hazard. Mater., 175 (2010) 298–303.

[52] W. C. Chen, H. Y. Lin, C. S. Yuan, C. H. Hung, Kinetic modeling on the adsorption of vapor-phase mercury chloride on activated carbon by thermogravimetric analysis, J. Air & Waste Manage. Assoc., 59 (2009) 227–235.

[53] D. Saha, S. G. Deng, Adsorption equilibrium and kinetics of CO_2, CH_4, N_2O, and NH_3 on ordered mesoporous carbon, J. Colloid Interf. Sci., 345 (2010) 402-409.

[54] S. Azizian, Kinetic models of sorption: a theoretical analysis, J. Colloid Interf. Sci., 276 (2004) 47–52.

[55] Y. S. Ho, Citation review of Lagergren kinetic rate equation on adsorption reactions, Scientometrics, 59 (2004) 171–177.

[56] L. C. Hall, L. C. Eagleton , A. Acrivos , T. Vermeulen , Pore and solid diffusion kinetics in fixed bed adsorption under constant pattern conditions, Ind. Eng. Chem. Fundamen., 5 (1966) 212–223.

[57] N. D. Hutson, R. T. Yang, Adsorption, J. Colloid Interf. Sci., 3 (2000) 189.

[58] P. D. Jadhav, R. V. Chatti, R. B. Biniwale, N. K. Labhsetwar, S. Devotta, S. S. Rayalu , Monoethanol amine modified zeolite 13X for CO_2 adsorption at different temperatures, Energy & Fuels 21 (2007) 3555–3559.

[59] P. Mishra, S. Edubilli, H. Uppara, B. Mandal, S. Gumma, effect of adsorbent history on adsorption characteristics of MIL-53(Al) metal organic framework, Langmuir 29 (2013) 12162−12167.

[60] P. Mishra, H. P. Uppara, B. Mandal, S. Gumma, Adsorption and separation of carbon dioxide using MIL-53(Al) metal-organic framework, Ind. Eng. Chem. Res., 53 (2014), 19747−19753.

[61] R. V. Siriwardance, M. S. Shen, E. P. Fisher, J. A. Poston, Adsorption of CO_2 on molecular sieves and activated carbon, Energy Fuels, 15(2001) 279-284.

[62] F. Dreisbach, R. Staudt, J. U. Keller, High pressure adsorption data of methane, nitrogen, carbon dioxide and their binary and ternary mixtures on activated carbon, Adsorption, 5(1999) 215.

[63] Y. Belmabkhout, R. S. Guerrero, A. Sayari, Adsorption of CO_2-containing gas mixtures over amine-bearing pore-expanded MCM-41 silica: application for gas purification, Ind. Eng. Chem. Res. 49 (2010) 359–365.

[64] Y.-S. Bae, O. K. Farha, J. T. Hupp, R. Q. Snurr, Enhancement of CO_2/N_2 selectivity in a metal-organic framework by cavity modification, J. Mater. Chem., 19 (2009) 2131–2134.

[65] S. Couck, J. F. M. Denayer, G. V. Baron, T. Rémy, J. Gascon, F. Kapteijn, F. An amine-functionalized MIL-53 metal-organic framework with large separation power for CO_2 and CH_4, J. Am. Chem. Soc. 131 (2009) 6326−6327.

[66] R. Banerjee, H. Furukawa, D. Britt, C. Knobler, M. O'Keeffe, O. M. Yaghi, Control of pore size and functionality in isoreticular zeolitic imidazolate frameworks and their carbon dioxide selective capture properties, J. Am. Chem. Soc. 131 (2009) 3875−3877.